

Tetra- and dinuclear manganese complexes of xanthene-bridged O,N,O-Schiff bases with 3-hydroxypropyl or 2-hydroxybenzyl groups: ligand substitution at a triply bridging site

Rina Ogawa,^a Takayoshi Suzuki,^{a,d} Masakazu Hirotsu,^{*b} Noriyuki Nishi,^c Yuu Shimizu,^c Yukinari Sunatsuki,^a Yoshio Teki,^c and Isamu Kinoshita^c

^a Department of Chemistry, Faculty of Science, Okayama University, Okayama 700-8530, Japan.

^b Department of Chemistry, Faculty of Science, Kanagawa University, 2946 Tsuchiya, Hiratsuka, Kanagawa 259-1293, Japan.

^c Division of Molecular Materials Science, Graduate School of Science, Osaka City University, 3-3-138 Sugimoto, Sumiyoshi-ku, Osaka 558-8585, Japan.

^d Research Institute for Interdisciplinary Science, Okayama University, Okayama 700-8530, Japan.

*Corresponding author. Tel.: +81 463 59 4111; Fax: +81 463 58 9684; e-mail: mhiro@kanagawa-u.ac.jp

Table S1. Crystallographic data for [3](ClO₄)₂, [4]BF₄, and 5

	[3](ClO ₄) ₂ ·2Pr ₂ O·5H ₂ O	[4]BF ₄ ·2CH ₂ Cl ₂ ·H ₂ O	5·2.6C ₇ H ₈ ·4.7H ₂ O
Empirical formula	C ₈₂ H ₁₀₆ Cl ₂ Mn ₂ N ₄ O ₂₅	C ₇₆ H ₇₇ BCl ₄ F ₄ Mn ₄ N ₄ O ₁₆	C _{104.20} H _{94.20} Mn ₂ N ₄ O _{14.70}
Formula weight	1728.53	1750.78	1747.51
Temperature/K	188	123	133
Wavelength/Å	0.7107	0.7107	0.7107
Crystal system	triclinic	monoclinic	tetragonal
Space group	<i>P</i> $\bar{1}$	<i>P</i> 2 ₁	<i>P</i> 4/ <i>n</i>
<i>a</i> /Å	11.0476(15)	13.2444(13)	27.3689(9)
<i>b</i> /Å	13.524(2)	17.0667(17)	27.3689(9)
<i>c</i> /Å	15.220(3)	16.6189(17)	12.0350(5)
<i>α</i> /°	103.322(6)	90	90
<i>β</i> /°	92.830(5)	91.476(3)	90
<i>γ</i> /°	105.832(4)	90	90
<i>V</i> /Å ³	2113.5(6)	3755.3(7)	9014.9(7)
<i>Z</i>	1	2	4
<i>D</i> _{calcd} /Mg·m ⁻³	1.358	1.548	1.288
<i>μ</i> (Mo Kα)/mm ⁻¹	0.440	0.880	0.348
<i>F</i> (000)	910	1796	3660
Crystal size/mm ³	0.30 × 0.20 × 0.10	0.24 × 0.21 × 0.06	0.21 × 0.17 × 0.14
Reflections collected	20828	36416	97041
Independent reflections	9616 (<i>R</i> _{int} = 0.0797)	16171 (<i>R</i> _{int} = 0.0469)	10238 (<i>R</i> _{int} = 0.0487)
Completeness to <i>θ</i>	99.1% (<i>θ</i> = 27.48°)	98.3% (<i>θ</i> = 27.48°)	99.1% (<i>θ</i> = 27.46°)
Max. and min. transmission	0.957 and 0.331	1.0000 and 0.8290	1.0000 and 0.9230
No. of data/restraints/parameters	9616/6/566	16171/1/1043	10238/15/590
Goodness of fit on <i>F</i> ²	1.052	1.031	1.107
Final <i>R</i> indices [<i>I</i> > 2σ(<i>I</i>)]	<i>R</i> 1 = 0.0899	<i>R</i> 1 = 0.0707	<i>R</i> 1 = 0.0685
<i>R</i> indices (all data)	w <i>R</i> 2 = 0.2755	w <i>R</i> 2 = 0.1913	w <i>R</i> 2 = 0.2002
Absolute structure parameter		0.480(11)	
Largest diff. peak and hole (e·Å ⁻³)	0.74 and -0.58	0.963 and -0.730	1.128 and -0.426

Table S2. Selected bond distances/Å and angles/° for [3](ClO₄)₂

Mn(1)–O(1)	2.236(3)	Mn(1)–O(4)	2.305(3)
Mn(1)–O(2)	1.857(3)	Mn(1)–O(4)*	1.927(3)
Mn(1)–N(1)	2.024(4)	Mn(1)–N(2)*	2.043(4)
Mn(1)–Mn(1)*	3.3269(13)		
O(1)–Mn(1)–O(2)	97.34(14)	O(1)–Mn(1)–O(4)	165.82(12)
O(1)–Mn(1)–O(4)*	90.35(13)	O(1)–Mn(1)–N(1)	82.48(15)
O(1)–Mn(1)–N(2)*	92.50(15)	O(2)–Mn(1)–O(4)	95.83(14)
O(2)–Mn(1)–O(4)*	171.98(15)	O(2)–Mn(1)–N(1)	89.78(15)
O(2)–Mn(1)–N(2)*	90.28(15)	O(4)–Mn(1)–O(4)*	76.74(13)
O(4)–Mn(1)–N(1)	92.36(15)	O(4)–Mn(1)–N(2)*	92.66(15)
O(4)*–Mn(1)–N(1)	93.50(15)	O(4)*–Mn(1)–N(2)*	87.09(15)
N(1)–Mn(1)–N(2)*	174.94(17)	Mn(1)–O(4)–Mn(1)*	103.26(13)
Mn(1)–O(4)–C(30)	123.8(3)	Mn(1)*–O(4)–C(30)	120.9(3)

Table S3. Selected bond distances/Å and angles/° for 5

Mn(1)–O(1)	1.8991(19)	Mn(1)–O(3)*	1.8941(19)
Mn(1)–O(2)	1.8862(18)	Mn(1)–O(4)*	1.8813(19)
Mn(1)–N(1)	1.999(2)	Mn(1)–N(2)*	1.991(2)
Mn(1)–Mn(1)*	8.1499(8)		
O(1)–Mn(1)–O(2)	178.78(8)	O(1)–Mn(1)–O(3)*	88.07(8)
O(1)–Mn(1)–O(4)*	88.88(8)	O(1)–Mn(1)–N(1)	89.69(8)
O(1)–Mn(1)–N(2)*	91.60(8)	O(2)–Mn(1)–O(3)*	90.92(8)
O(2)–Mn(1)–O(4)*	92.13(8)	O(2)–Mn(1)–N(1)	90.97(8)
O(2)–Mn(1)–N(2)*	87.71(8)	O(3)*–Mn(1)–O(4)*	176.91(8)
O(3)*–Mn(1)–N(1)	89.29(9)	O(3)*–Mn(1)–N(2)*	89.41(9)
O(4)*–Mn(1)–N(1)	90.24(9)	O(4)*–Mn(1)–N(2)*	91.14(9)
N(1)–Mn(1)–N(2)*	178.13(9)		

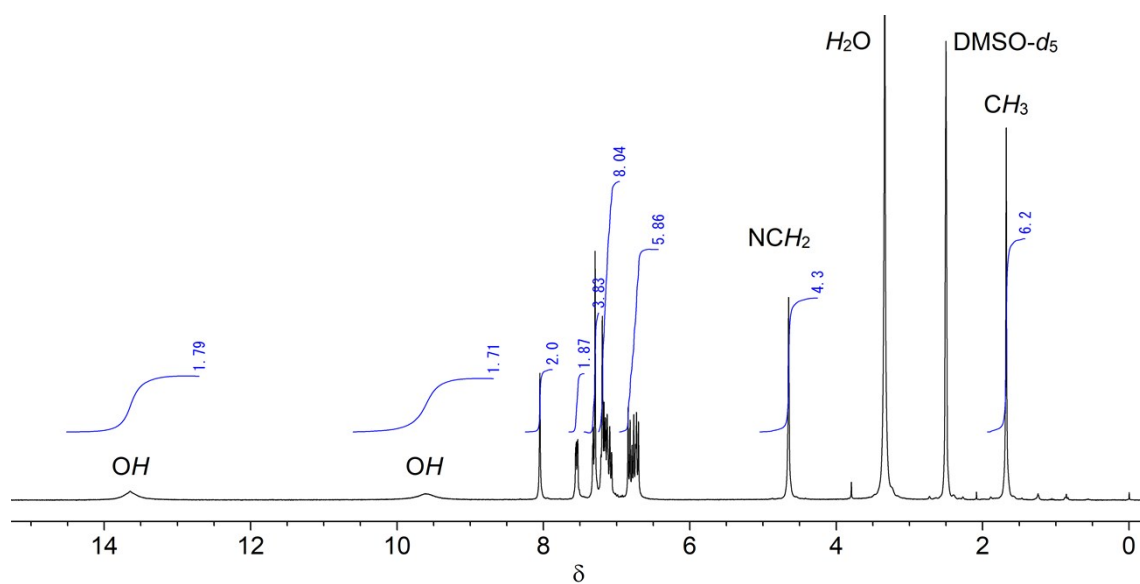


Fig. S1. ^1H NMR (300 MHz, $\text{DMSO-}d_6$) spectrum of H_4L^2 .

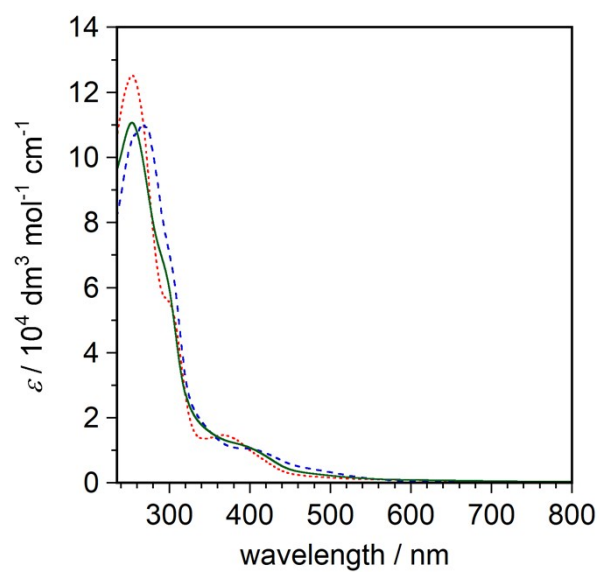


Fig. S2. Absorption spectra of tetramanganese complexes **1** (.....), **2** (- - -), and $[\mathbf{4}]\text{BF}_4$ (—) in dichloromethane.

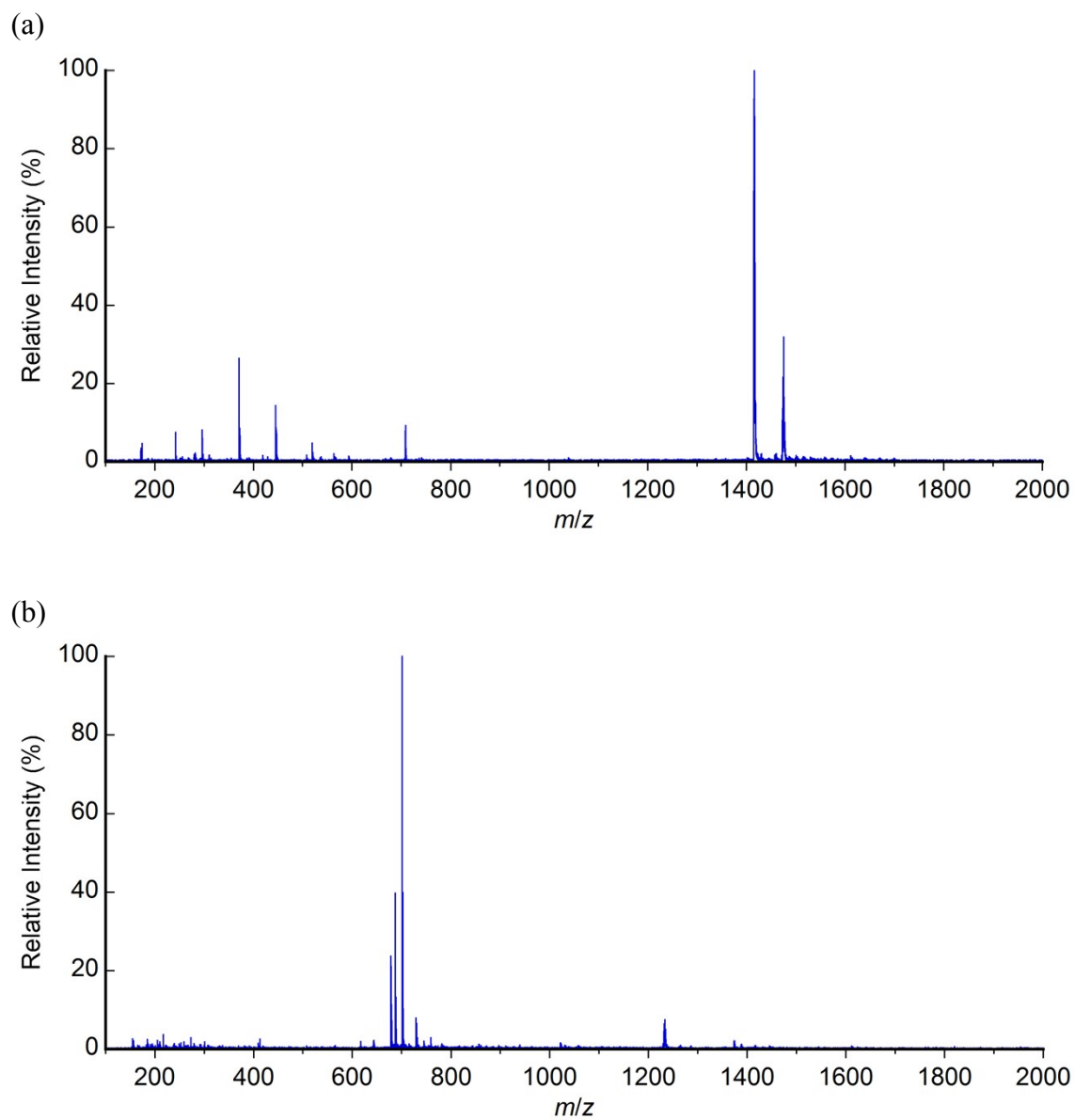


Fig. S3. ESI mass spectra of [4](BF₄) in (a) dichloromethane and (b) methanol.

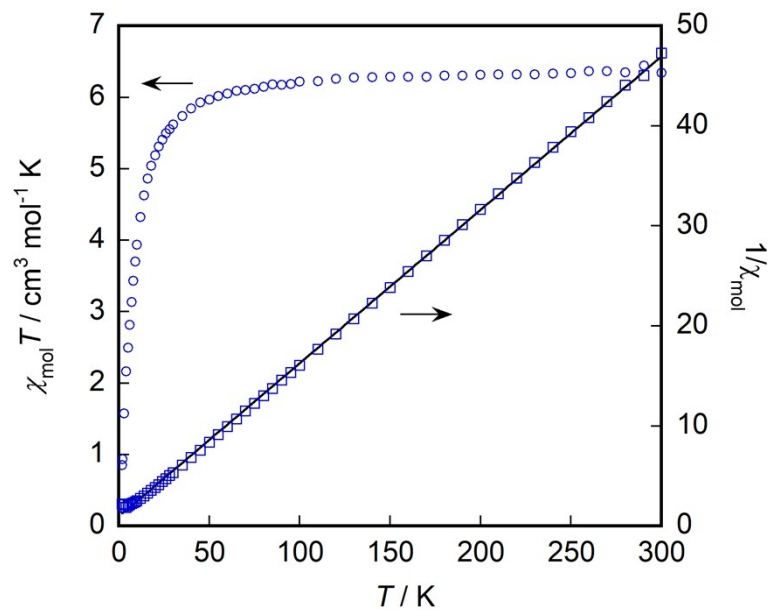


Fig. S4. Temperature dependence of χT and $1/\chi$ for $[3](\text{ClO}_4)_2$. Solid lines represent the least-squares fits of the data to the model described in the text.

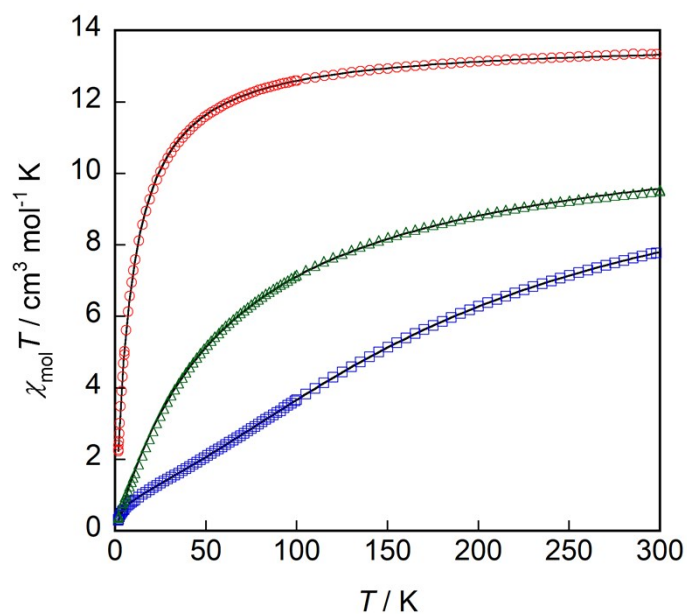


Fig. S5. Temperature dependence of χT for **1** (\circ), **2** (\square), and $[4](\text{BF}_4)$ (\triangle). Solid lines represent the least-squares fits of the data to the model described in the text.

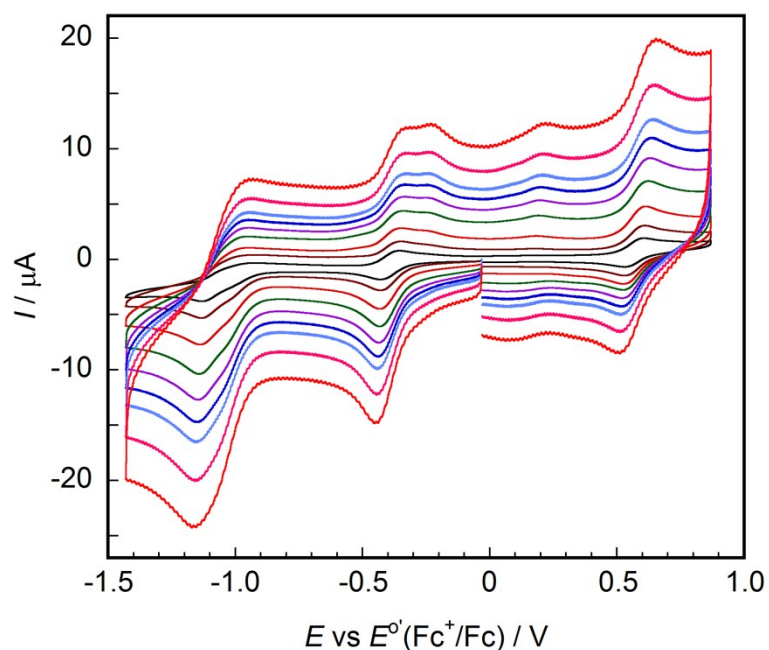


Fig. S6. Cyclic voltammograms of [4]PF₆ (2.3×10^{-4} M) in CH₂Cl₂ containing 0.1 M Bu₄NPF₆: scan rate, 20 (black), 50 (dark brown), 100 (red brown), 200 (green), 300 (purple), 400 (blue), 500 (light blue), 700 (pink), 1000 (red) mV s⁻¹; working electrode, glassy carbon; auxiliary electrode, platinum wire; reference electrode, Ag/Ag⁺. Potentials are versus ferrocenium/ferrocene (Fc⁺/Fc).

Reference

- 1) M. Hirotsu, Y. Shimizu, N. Kuwamura, R. Tanaka, I. Kinoshita, R. Takada, Y. Teki and H. Hashimoto, *Inorg. Chem.*, 2012, **51**, 766–768.